

Combining Pyrazolate and N-Heterocyclic Carbene Coordination Motifs: Synthesis and Characterization of a Double-Crowned Silver Complex

Ulrich J. Scheele, Maria Georgiou, Michael John, Sebastian Dechert, and Franc Meyer*

Institut für Anorganische Chemie, Georg-August-Universität Göttingen, Tammannstrasse 4, D-37077 Göttingen, Germany

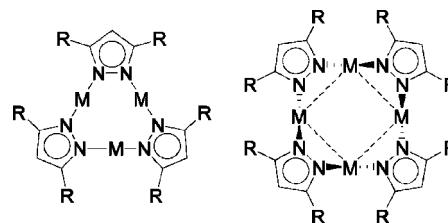
Received May 28, 2008

Reaction of Ag_2O with the N-heterocyclic carbene (NHC) precursors 3,5-bis[3-(2,4,6-trimethylphenyl)imidazolium-1-ylmethyl]-1*H*-pyrazole bishexafluorophosphate (**1a**) and 3,5-bis[3-(2,6-diisopropylphenyl)imidazolium-1-ylmethyl]-1*H*-pyrazole bishexafluorophosphate (**1b**) yielded silver(I) complexes **2** and **3**, respectively. X-ray crystallography revealed a tetranuclear dimeric solid state structure in the case of **2**, whereas an unprecedented octanuclear tetrameric “double-crown”-like structure was found for **3**, presumably due to the slightly bulkier ligand. Unlike **2**, complex **3** is not stable in solution but in equilibrium with tetranuclear and hexanuclear complexes **4** and **5**, respectively. The identity of those species could be elucidated by detailed NMR spectroscopic studies (^1H , ^{13}C , ^{15}N , ^{109}Ag , and DOSY experiments), which also provide valuable benchmark data for correlating $^1J_{\text{AgN}}$ couplings and ^{109}Ag chemical shifts with structural information.

Introduction

N-Heterocyclic carbenes (NHCs) and their organometallic coordination chemistry are a well-established and flourishing field of research.¹ Among the NHC complexes, silver(I) derivatives have attracted much attention,² especially because of their use as carbene transfer reagents.^{3,4} The first example of a silver(I) NHC complex was prepared from the free carbene,⁵ but deprotonation of ligand precursors, mostly imidazolium salts, by basic silver(I) salts provides a more convenient access without the need of strictly anaerobic conditions, and therefore this route is quite popular.⁴ The silver(I) NHC complexes are highly interesting themselves, since a large variety of structural motifs can be realized by variation of reaction conditions or anions and by alteration of electronic and steric properties of the NHCs.^{4,6,7} This is usually accomplished by variation of the N-bound substituents of the imidazolium moiety. Examples range from simple alkyl or aryl groups to functional groups that

Chart 1. Trimeric and Tetrameric Pyrazolate Complexes



provide additional donor atoms, eventually giving rise to pincer or chelate NHC complexes.^{6,7} Several recent reports deal with pyrazolyl-substituted silver NHC complexes,^{8–10} which offer potential applications as new luminescent materials^{10,11} or as starting materials for transmetalation, yielding highly preorganized bimetallic complexes.¹²

Luminescence properties have also been of major interest in the investigation of homoleptic silver(I) pyrazolate complexes.¹³ A common structural feature of many coinage metal pyrazolate complexes is a nine-membered $[\text{M}(\mu\text{-pz})_3]$ ring, the geometry being induced by the preferred linear coordination around the metal ions and the 120° $\text{M}-\text{N}-\text{N}$ angle (Chart 1).¹⁴ These trimeric units can be further stabilized by intra- and intermo-

* Corresponding author. Tel: +49 551 393012. Fax: +49 551 393063. E-mail: franc.meyer@chemie.uni-goettingen.de.

(1) (a) Bourissou, D.; Guerret, O.; Gabbai, F. P.; Bertrand, G. *Chem. Rev.* **2000**, *100*, 39–91. (b) Arnold, P. L. *Heteroat. Chem.* **2002**, *13*, 534–539. (c) Herrmann, W. A. *Angew. Chem., Int. Ed.* **2002**, *41*, 1290–1309. (d) Peris, E.; Crabtree, R. H. *Coord. Chem. Rev.* **2004**, *248*, 2239–2246. (e) Scott, N. M.; Nolan, S. P. *Eur. J. Inorg. Chem.* **2005**, *181*, 5–1828. (f) Sommer, W. J.; Weck, M. *Coord. Chem. Rev.* **2007**, *251*, 860–873. (g) Kühl, O. *Chem. Soc. Rev.* **2007**, *36*, 592–607.

(2) (a) Garrison, J. C.; Tessier, C. A.; Youngs, W. J. *J. Organomet. Chem.* **2005**, *690*, 6008–6020. (b) Samantaray, M. K.; Katiyar, V.; Roy, D.; Pang, K. L.; Nanavati, H.; Stephen, R.; Sunoj, R. B.; Ghosh, P. *Eur. J. Inorg. Chem.* **2006**, *297*, 5–2984. (c) Lee, C. K.; Vasam, C. S.; Huang, T. W.; Wang, H. M. J.; Yang, R. Y.; Lee, C. S.; Lin, I. J. B. *Organometallics* **2006**, *25*, 3768–3775. (d) Kascatan-Nebioglu, A.; Panzner, M. J.; Tessier, C. A.; Cannon, C. L.; Youngs, W. J. *Coord. Chem. Rev.* **2007**, *251*, 884–895.

(3) Wang, H. M. J.; Lin, I. J. B. *Organometallics* **1998**, *17*, 972–975.

(4) Lin, I. J. B.; Vasam, C. S. *Coord. Chem. Rev.* **2007**, *251*, 642–670.

(5) Arduengo III, A. J.; Dias, H. V. R.; Calabrese, J. C.; Davidson, F. *Organometallics* **1993**, *12*, 3405–3409.

(6) Garrison, J. C.; Youngs, W. J. *Chem. Rev.* **2005**, *105*, 3978–4008.

(7) Lin, I. J. B.; Vasam, C. S. *Comments Inorg. Chem.* **2004**, *25*, 75–129.

(8) (a) Wang, R.; Twamley, B.; Shreeve, J. M. *J. Org. Chem.* **2006**, *71*, 426–429. (b) Chiu, P. L.; Chen, C. Y.; Lee, C. C.; Hsieh, M. H.; Chuang, C. H.; Lee, H. M. *Inorg. Chem.* **2006**, *45*, 2520–2530.

(9) Zhou, Y.; Chen, W. *Organometallics* **2007**, *26*, 2742–2746.

(10) Zhou, Y.; Zhang, X.; Chen, W.; Qiu, H. *J. Organomet. Chem.* **2008**, *693*, 205–215.

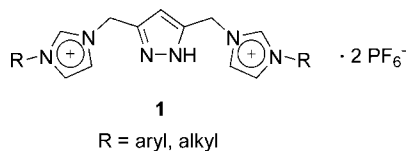
(11) Omary, M. A.; Rawashdeh-Omary, M. A.; Diyabalanage, H. V. K.; Dias, H. V. R. *Inorg. Chem.* **2003**, *42*, 8612–8614.

(12) Scheele, U. J.; John, M.; Dechert, S.; Meyer, F. *Eur. J. Inorg. Chem.* **2008**, *37*, 3–377.

(13) (a) Omary, M. A.; Rawashdeh-Omary, M. A.; Gonsler, M. W. A.; Elbjairami, O.; Grimes, T.; Cundari, T. R.; Diyabalanage, H. V. K.; Gamage, C. S. P.; Dias, H. V. R. *Inorg. Chem.* **2005**, *44*, 8200–8210. (b) Dias, H. V. R.; Diyabalanage, H. V. K.; Gamage, C. S. P. *Chem. Commun.* **2005**, 1619–1621.

(14) Murray, H. H.; Raptis, R. G., Jr. *Inorg. Chem.* **1988**, *27*, 26–33.

Chart 2. Ligand Precursors 1



lecular metal–metal contacts^{15,16} as well as π -acid/base interactions.¹⁷ However, increased steric bulk of substituents on the 3,5-positions of the pyrazole, e.g., *tert*-butyl, may lead to the formation of tetrameric structures (Chart 1), as was recently shown for $[\text{Ag}(\mu\text{-}3,5\text{-}t\text{-Bu}_2\text{pz})]_4$.¹⁸ This is the only tetrameric silver pyrazolate that has been structurally characterized so far,¹⁸ even though this class of compounds has been mentioned much earlier.¹⁹ In this work we present a silver(I) complex that combines the rare theme of such a tetrameric pyrazolate-bridged structure with an envelope of peripheral bis(NHC) moieties.

Results

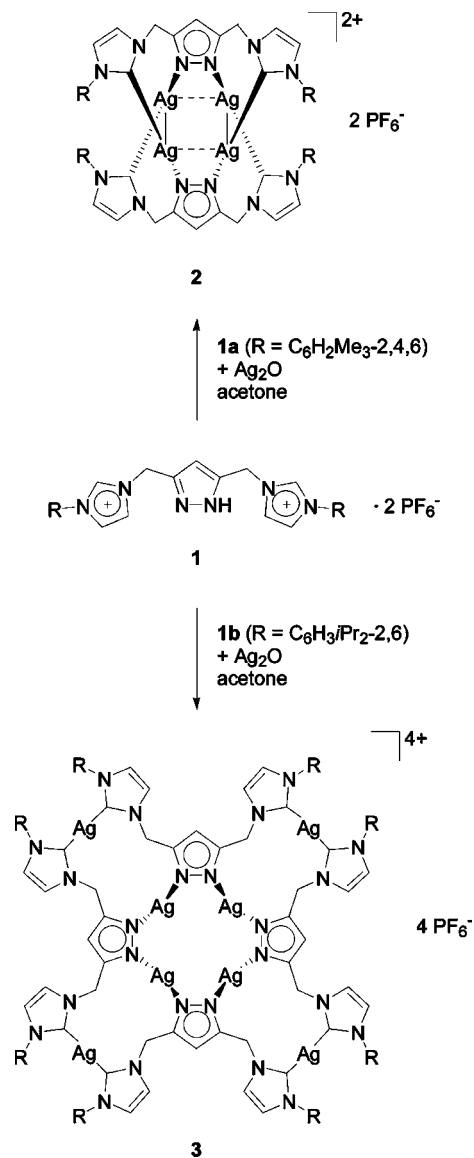
Ligand precursors **1** (Chart 2) combine imidazole and potentially bridging pyrazole moieties. Several possible synthetic strategies for the preparation of these compounds have recently been published by our group^{12,20} and others.^{9,10,21}

Reaction of silver(I) oxide with these ligand precursors yields silver(I) complexes. In our previous work focused on palladium complexes,¹² the intermediate silver complexes were not characterized in detail but were just used as transmetalation reagents. Composition and structures of the silver complexes were initially assumed to be very similar to those published.^{9,10} However, when we recorded NMR spectra of the crude reaction products of **1a** and **1b** with Ag_2O , we found major differences from the reported data and unusual solution spectroscopic signatures. This was surprising, and we therefore decided to investigate this phenomenon in more detail.

The ligand precursor **1a** was used to synthesize the silver(I) complex **2** (Scheme 1). This complex could be crystallized by diffusion of diethyl ether into an acetone solution. X-ray crystallography revealed the molecular structure of compound **2** (Figure 1). A crystallographically imposed C_i symmetry is found in **2**, and the silver atoms are arranged close to rectangular ($\text{Ag}\cdots\text{Ag}\cdots\text{Ag}$ angles around 90°). $\text{Ag}\cdots\text{Ag}$ distances (3.0452(3) and 3.3770(3) Å) are indicative of a pairwise $d^{10}\text{-}d^{10}$ interaction.²² Each silver atom in **2** is coordinated almost linearly by one pyrazolate-N and one NHC of the other ligand.

The ^1H NMR spectrum of **2** in acetone- d_6 contains a single resonance for the pyrazole proton (CH^{pz}), two AB doublets ($^2J_{\text{HH}} = 15.0$ Hz) for the methylene groups, and two triplets ($^3J_{\text{HH}} \approx ^4J_{\text{HAg}} \approx 1.5$ Hz) for the imidazole protons. None of these signals show dynamic line broadening between 25 and -50 °C,

Scheme 1. Synthesis of Silver Complexes 2 and 3



indicating the two halves of the ligand remain equivalent on the NMR time scale. All five signals from the ligand core are J-coupled to a single silver resonance at 618.2 ppm, meaning

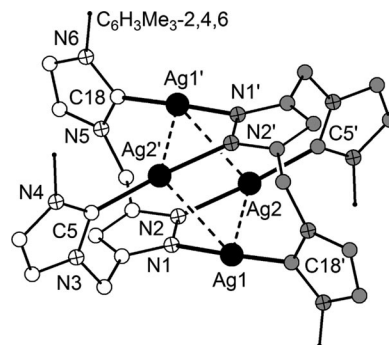


Figure 1. Plot of the molecular structure of **2**. For the sake of clarity all hydrogen atoms, PF_6^- ions, and solvent molecules have been omitted. Selected bond lengths [Å] and angles [deg]: Ag1-N1 2.084(2), $\text{Ag1-C18}'$ 2.057(2), Ag2-N2 2.103(2), $\text{Ag2-C5}'$ 2.075(2), $\text{Ag1}\cdots\text{Ag2}$ 3.3770(3), $\text{Ag1}\cdots\text{Ag2}'$ 3.0452(3); $\text{N1-Ag1-C18}'$ 178.58(8), $\text{N2-Ag2-C5}'$ 175.62(9), $\text{Ag2}\cdots\text{Ag1}\cdots\text{Ag2}'$ 90.477(7), $\text{Ag1}\cdots\text{Ag2}\cdots\text{Ag1}'$ 89.523(7). Symmetry transformation used to generate equivalent atoms ($'$): $1-x, 1-y, 1-z$.

(15) (a) Meyer, F.; Jacobi, A.; Zsolnai, L. *Chem. Ber.* **1997**, *130*, 1441–1447. (b) Li, R. *Acta Crystallogr.* **2007**, *E63*, m1640. (c) Dias, H. V. R.; Polach, S. A.; Wang, Z. *J. Fluorine Chem.* **2000**, *103*, 163–169.

(16) Mohamed, A. A.; Perez, L. M., Jr. *Inorg. Chim. Acta* **2005**, *358*, 1657–1662.

(17) (a) Dias, H. V. R.; Gamage, C. S. P.; Keltner, J.; Diyabalanage, H. V. K.; Omari, I.; Eyobo, Y.; Dias, N. R.; Roehr, N.; McKinney, L.; Poth, T. *Inorg. Chem.* **2007**, *46*, 2979–2987. (b) Dias, H. V. R.; Gamage, C. S. P. *Angew. Chem., Int. Ed.* **2007**, *46*, 2192–2194.

(18) Yang, G.; Raptis, R. G. *Inorg. Chim. Acta* **2007**, *360*, 2503–2506.

(19) Trofimenko, S. *Chem. Rev.* **1972**, *72*, 497–509.

(20) Scheele, U. J. Diploma thesis, Georg-August-Universität Göttingen, 2004.

(21) Jeon, S.-J.; Waymouth, R. M. *Dalton Trans.* **2008**, 437–439.

(22) (a) Jansen, M. *Angew. Chem., Int. Ed.* **1987**, *26*, 1098–1110. (b) Che, C.-M.; Lai, S.-W. *Coord. Chem. Rev.* **2005**, *249*, 1296–1309.

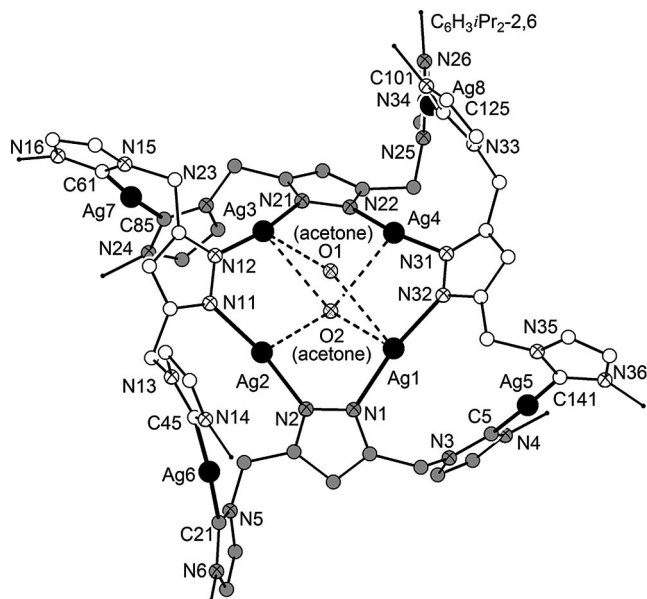


Figure 2. Plot of the molecular structure of **3**. For the sake of clarity all hydrogen atoms and PF_6^- ions have been omitted. Selected bond lengths [Å] and angles [deg]: Ag1–N1 2.102(4), Ag1–N32 2.107(5), Ag1...O1 2.908(7), Ag1...O2 2.906(4), Ag2–N2 2.093(4), Ag2–N11 2.093(5), Ag2...O1 3.134(8), Ag2...O2 2.921(4), Ag3–N12 2.105(4), Ag3–N21 2.101(4), Ag3...O1 3.009(6), Ag3...O2 3.033(5), Ag4–N22 2.086(4), Ag4–N31 2.086(4), Ag4...O1 3.081(7), Ag4...O2 2.877(5), Ag5–C5 2.082(6), Ag5–C141 2.087(6), Ag6–C21 2.094(6), Ag6–C45 2.112(7), Ag7–C61 2.083(6), Ag7–C85 2.093(6), Ag8–C101 2.100(6), Ag8–C125 2.074(6), Ag1...Ag2 3.6996(5), Ag1...Ag3 5.0862(6), Ag1...Ag4 3.5744(6), Ag1...Ag5 4.0833(6), Ag2...Ag3 3.5706(6), Ag2...Ag4 5.1637(6), Ag2...Ag6 3.9940(7), Ag3...Ag4 3.6754(5), Ag3...Ag7 4.0033(5), Ag4...Ag8 3.7764(6); N1–Ag1–N32 170.58(17), N2–Ag2–N11 171.32(17), N12–Ag3–N21 170.91(17), N22–Ag4–N31 171.22(18), C5–Ag5–C141 176.2(3), C21–Ag6–C45 174.4(3), C61–Ag7–C85 175.7(2), C101–Ag8–C125 173.9(2).

that all silver atoms are equivalent and simultaneously bound to the pyrazolate-N and NHC. All NMR spectra are in agreement with the solid state structure of **2** and with reports of related compounds;^{9,10} it can therefore be assumed that the rigid structure of **2** is retained in solution.

NMR spectra of the product derived from **1b** are more complicated and show the presence of several species. In order to clarify the situation, it was first of all necessary to crystallize the product and determine the molecular structure in the solid state. Colorless crystals of the silver(I) complex **3** were likewise obtained by diffusion of diethyl ether into an acetone solution. The identity of **3** was then elucidated by X-ray crystallography. Its molecular structure may be described as a “double crown” with inner N-coordinated and outer C-coordinated silver(I) atoms and is depicted in Figure 2. The central core of the complex is made up of four silver(I) atoms in a nearly square-planar arrangement that are bridged by pyrazolate ligands situated alternately above and below the plane in a S_4 -symmetric fashion. This saddle-like geometry is known from the related compound $[\text{Ag}(\mu\text{-}3,5\text{-}t\text{-Bu}_2\text{pz})_4]_4$.¹⁸ Ag...Ag distances range from 3.5706(6) to 3.6996(5) Å, considerably longer than the sum of the van der Waals radii (3.44 Å),²³ thereby clearly indicating the absence of any Ag–Ag contacts. Instead, there seems to be a weak interaction with the oxygen atoms of two acetone molecules located on either side of the Ag_4 plane ($d(\text{Ag}–\text{O}) = 2.877(5)–3.134(8)$

Table 1. Selected NMR Data

	2 ^a	3 ^a	4 ^b	5 ^b
¹³ C/ppm	177.6	180.0/183.4 ^c	179.4	181.0
¹ J _{13C¹⁰⁹Ag/Hz}	269	210/211 ^c	272	209
¹ J _{13C¹⁰⁷Ag/Hz}	233	181/183 ^c	236	181
¹⁵ N ^{pz} /ppm	–109.4	–117.6/–116.4	–109.8	–116.1
¹ J _{15N^{Ag}/Hz^d}	79	97	72	96
¹⁰⁹ Ag/ppm	618.2 ^e	469.7/636.5 ^g	614.8 ^e	503.6 ^f /651.1 ^g

^a $T = -50$ °C. ^b $T = +25$ °C. ^c Values for the two nonequivalent halves of the ligand. ^d Average of ¹J_{15N¹⁰⁹Ag and ¹J_{15N¹⁰⁷Ag. ^e C–Ag–N. ^f N–Ag–N. ^g C–Ag–C.}}

Å). The Ag–N bond lengths (2.086(4)–2.107(5) Å, average 2.097 Å) and N–Ag–N angles (170.58(17)–171.32(17)°, average 171.01°) in **3** are very similar to those of $[\text{Ag}(\mu\text{-}3,5\text{-}t\text{-Bu}_2\text{pz})_4]_4$.

In **3**, all neighboring ligand molecules are further linked through an additional bis(NHC)-bound silver(I) ion. Thus, an array of four bis(NHC) silver(I) motifs surrounds the central pyrazolate-based silver core (Figure 2). Ag–C bond lengths (2.074(6)–2.112(7) Å, average 2.091 Å) and C–Ag–C angles (173.9(2)–176.2(3)°, average 175.1°) are well within the expected range.⁶ Due to the bulky aryl substituents, the two Ag-bound imidazole rings are twisted out of plane by approximately 45°, resulting in $\text{C}^{\text{pz}}\text{--CH}_2\text{--N}^{\text{im}}\text{--C}^{\text{carbene}}$ dihedral angles that are remarkably different for the two halves of the ligand (average of 72° and 127°).

To characterize **3** by NMR, a single crystal was dissolved in acetone-*d*₆ at –50 °C. The ¹H NMR spectrum shows a single CH^{pz} resonance, but, different from **2**, four CH_2 doublets, four imidazole, and a double set of aryl resonances from the two inequivalent ligand halves. The two sets of signals do, however, slowly (0.25 s^{–1}) interconvert at –50 °C, are strongly broadened at 0 °C, and partially coalesced at 25 °C (see Figure S3 in the Supporting Information). In the tetrameric structure of **3** this would correspond to a barrier of about 13.5 kcal/mol for the simultaneous inversion of all ligand molecules, presumably through a S_4 -symmetric transition state.

In contrast to complex **2**, the pyrazole and imidazole protons in **3** are *J*-coupled to two different ¹⁰⁹Ag resonances at 469.7 and 636.5 ppm, respectively. Furthermore, as shown in Table 1, the carbene ¹³C and pyrazole ¹⁵N resonances and their splittings due to the bound isotopes ¹⁰⁹Ag and ¹⁰⁷Ag are remarkably different in **2** and **3**. Thus, NMR data confirm the heteroleptic C–Ag–N versus homoleptic N–Ag–N plus C–Ag–C bonding situation found in the solid state.

Whereas the NMR spectra of **2** in acetone are nearly independent of temperature between –50 and 50 °C and indefinitely stable, in the single-crystal sample of **3** at 25 °C we observed slow formation of two new products (named **4** and **5** hereafter) while the amount of **3** decreases (see again Figure S3 in the Supporting Information). The final ratio of **3**, **4**, and **5** at equilibrium, which was typically reached within a few hours, depends on the original concentration of **3** (where more of **3** is retained at higher concentrations). ¹H NMR spectra of the mixture resemble that of the crude product before crystallization.

While the peaks of **3** are mostly broad at 25 °C (see above), components **4** and **5** each show a single narrow resonance for one CH^{pz} and two imidazole protons. The CH^{pz} resonance of **5** is, however, shifted remarkably downfield to 7.19 ppm vs 6.63 ppm in **3** and 6.56 ppm in **4**. The CH_2 group appears as an AB system in **4**, but as a singlet in **5**. As shown in Table 1, the key ¹³C, ¹⁵N, and ¹⁰⁹Ag spectral parameters of **4** resemble that of **2**, while the parameters of **5** are more closely related to **3**.

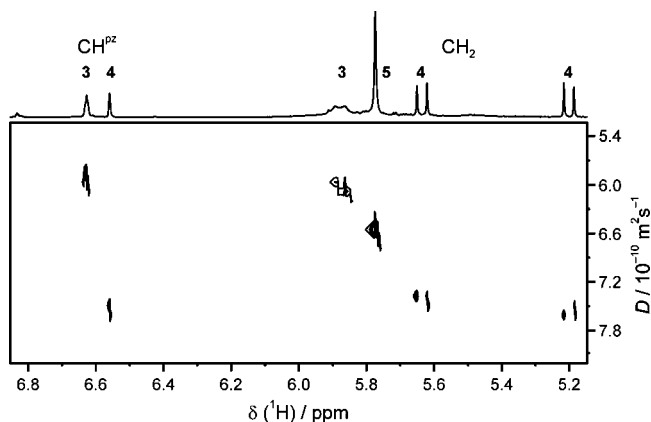


Figure 3. Part of the DOSY spectrum of the mixture obtained at RT from crystalline **3** in acetone- d_6 showing the signals for the CH^{pz} and CH_2 groups. (The CH^{pz} proton in **5** resonates at 7.19 ppm and is not shown here.)

In order to distinguish **3**, **4**, and **5** by their molecular size, we measured diffusion coefficients in the mixed sample using DOSY NMR. As shown in Figure 3, the diffusion coefficient D of **4** ($(7.6 \pm 0.1) \times 10^{-10} \text{ m}^2 \text{ s}^{-1}$) is substantially higher than that of **3** ($(5.8 \pm 0.1) \times 10^{-10} \text{ m}^2 \text{ s}^{-1}$), while that of **5** is in between ($(6.4 \pm 0.1) \times 10^{-10} \text{ m}^2 \text{ s}^{-1}$). In spherical particles of a given mass density and solvent viscosity, the diffusion coefficient is proportional to the inverse cubic root of the mass of the particle. From this relation, we estimated the relative molecular mass of **3**, **4**, and **5** as 1.0:0.47:0.81.

Discussion

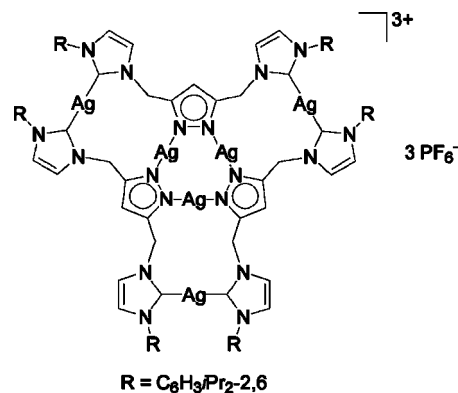
3,5-Substituted pyrazoles may form intermolecular hydrogen bonds, giving rise to cyclic $[\text{H}(\mu\text{-}3,5\text{-R}_2\text{pz})_x]$ structures.^{24,25} In the case of sterically demanding residues R, e.g., phenyl, tetrameric structures are preferred.²⁵ In contrast, group 11 complexes of this ligand type, where the distance between the pyrazole-N atoms is increased, tend to form planar trimeric structures.^{14,16} As silver gives rise to longer M–N bonds than other coinage metals, massive steric hindrance seems necessary to enforce the tetrameric, folded geometry.¹⁸ Although the substituents at positions 3 and 5 of the pyrazole in **3** are flexible and only moderately bulky, the tetrameric structure is observed. Possibly, the silver pyrazolate core of **3** is largely stabilized by the additional interligand silver–NHC linkages in the periphery of the central core.

Starting from the slightly modified ligand **1a**, but using otherwise identical conditions, complex **2** crystallized in a completely different, dimeric structure with heteroleptically coordinated silver ions. This structural motif has recently been reported for related ligands,^{9,10} with minor structural deviations presumably arising from different crystallization conditions, counterions, and solvents as well as temperature effects. Formation of the different structures **2** and **3** seems remarkable, as **1a** and **1b** differ only by the substituents ($\text{C}_6\text{H}_2\text{Me}_3\text{-}2,4,6$ vs $\text{C}_6\text{H}_3\text{Pr}_2\text{-}2,6$) on the imidazole rings. These residues are fairly remote from the pyrazolate core and electronically very similar,

(24) (a) Foces-Foces, C. N.; Alkorta, I.; Elguero, J. *Acta Crystallogr.* **2000**, B56, 1018–1028. (b) Infantes, L.; Motherwell, S. *Struct. Chem.* **2004**, 15, 173–184.

(25) (c) Claramunt, R. M.; Cornago, P.; Torres, V.; Pinilla, E.; Torres, M. R.; Samat, A.; Lokshin, V.; Valés, M.; Elguero, J. *J. Org. Chem.* **2006**, 71, 6881–6891. (d) Sachse, A.; Penkova, L.; Noël, G.; Dechert, S.; Varzatskii, O. A.; Fritsky, I. O.; Meyer, F. *Synthesis* **2008**, 800–806. Raptis, R. G.; Staples, R. J.; King, C., Jr *Acta Crystallogr.* **1993**, C49, 1716–1719.

Chart 3. Proposed Molecular Structure of **5**



suggesting that the tetrameric structure **3** is mainly a result of the sterically slightly more demanding wingtips in **1b**. Since the structural motif observed for **2** with its heteroleptic C–Ag–N coordination appears to be generally favored in the absence of steric constraints, the relative stability of homoleptic N–Ag–N and C–Ag–C coordination modes should be slightly lower compared to the heteroleptic situation.

The situation is more complex in solution, where we could show by NMR spectroscopy that **3** is only one of three species that slowly equilibrate at room temperature. Comparison of chemical shifts of the pyrazolate-N and silver ions, coupling constants $^1J_{\text{AgC}}$ and $^1J_{\text{AgN}}$, and diffusion coefficients D lead to the conclusion that species **4** is dimeric and isostructural to **2**. The exact nature of the third component, **5**, remains speculative, although the NMR data suggest it may represent the trimeric pyrazolate core with additional silver–NHC linkages (Chart 3). A rather flat overall structure would also explain the appearance of a narrow singlet for the CH_2 groups instead of AB doublets. Furthermore, this structure would be in line with nine-membered $[\text{M}(\mu\text{-pz})_3]$ rings being the most common motif for pyrazolate complexes of coinage metals in oxidation state +1.

The present work underlines the significance of heteronuclear NMR in silver pyrazolate and carbene chemistry. Coupling constants $^1J_{\text{AgC}}$ have been reported for a range of silver NHC complexes.⁶ In C–Ag–X (X = O, Cl) systems, the values tend to be some 30% larger than in the parent C–Ag–C systems,^{26,27} indicating a strengthening of the Ag–NHC bond upon heteroleptic coordination. This is in full agreement with the C–Ag–N bonding situation in **2** and **4**, where an increase of 30% in $^1J_{\text{AgC}}$ of the remaining NHC ligand is also observed.²⁸ The Ag–pyrazolate bond, on the other hand, weakens upon heteroleptic coordination, as may be deduced from a 20–25% decreased $^1J_{\text{AgN}}$ coupling constant in **2** and **4** versus **3** and **5**. Another useful indicator for the coordination sphere of silver is the observed ^{109}Ag chemical shift; C–Ag–N bound silver resonates more than 100 ppm downfield of N–Ag–N and is distinguished from C–Ag–C

(26) (a) Weigl, K.; Köhler, K.; Dechert, S.; Meyer, F. *Organometallics* **2005**, 24, 4049–4056. (b) Van Veldhuizen, J. J.; Campbell, J. E.; Giudici, R. E.; Hoveyda, A. H. *J. Am. Chem. Soc.* **2005**, 127, 6877–6882. (c) Herrmann, W. A.; Schneider, S. K.; Öfele, K.; Sakamoto, M.; Herdtweck, E. *J. Organomet. Chem.* **2004**, 689, 2441–2449. (d) Pytkowicz, J.; Roland, S.; Mangeney, P. *J. Organomet. Chem.* **2001**, 631, 157–163.

(27) Rammial, T.; Abernethy, C. D.; Spicer, M. D.; McKenzie, I. D.; Gay, I. D.; Clyburne, J. A. C. *Inorg. Chem.* **2003**, 42, 1391–1393.

(28) Note that a similar situation was found in a complex related to **2** and **4**. In ref 9 two singlets at 178.1 and 175.8 ppm were found in the ^{13}C NMR spectra for NHC carbon atoms, translating to a coupling of 230 Hz (not 23 Hz as reported). This is probably due to an unresolved coupling of $^1J_{^{13}\text{C}^{109}\text{Ag}}$ and $^1J_{^{13}\text{C}^{107}\text{Ag}}$; the given explanation (“anionic pyrazolate is not fully electron-delocalized”) may be doubted.

Table 2. Summary of X-ray Crystallographic Data for Complexes **2** and **3**

	2	3
empirical formula	C ₅₈ H ₆₂ Ag ₄ N ₁₂ ²⁺ , 2 PF ₆ ⁻ , 4 C ₃ H ₆ O	C ₁₄₆ H ₁₈₄ Ag ₈ N ₂₄ O ₂₄ ⁴⁺ , 4 PF ₆ ⁻
fw	1880.93	3750.01
cryst size [mm]	0.39 × 0.24 × 0.22	0.40 × 0.33 × 0.30
cryst syst	triclinic	triclinic
space group	<i>P</i> $\bar{1}$ (No. 2)	<i>P</i> $\bar{1}$ (No. 2)
<i>a</i> [Å], α [deg]	12.5681(5), 63.361(3)	19.2514(4), 80.184(2)
<i>b</i> [Å], β [deg]	12.9967(5), 68.893(3)	21.4494(5), 82.059(2)
<i>c</i> [Å], γ [deg]	14.3012(6), 80.629(3)	23.7189(5), 77.330(2)
<i>V</i> [Å ³]	1947.95(14)	9364.0(4)
ρ_{calcd} [g cm ⁻³]	1.603	1.330
<i>Z</i>	1	2
<i>F</i> (000)	948	3792
μ [mm ⁻¹]	1.114	0.925
<i>T</i> _{max} / <i>T</i> _{min}	0.8155/0.6622	
<i>hkl</i> range	-14 - 16, \pm 16, \pm 18	\pm 23, \pm 26, \pm 28
θ range [deg]	1.68-26.99	1.22-25.79
no. measd reflns	23 394	103 102
no. unique reflns [<i>R</i> _{int}]	8462 [0.0278]	35 310 [0.0380]
no. obsd reflns <i>I</i> > 2 σ (<i>I</i>)	7426	27 609
no. refined params/restraints	479/0	1847/192
goodness-of-fit	1.026	1.030
<i>R</i> ₁ , <i>wR</i> ₂ (<i>I</i> > 2 σ (<i>I</i>))	0.0288/0.0722	0.0562/0.1506
<i>R</i> ₁ , <i>wR</i> ₂ (all data)	0.0347/0.0745	0.0706/0.1564
resid el dens [e Å ⁻³]	1.048/-0.955	1.446/-1.333

by an upfield shift of about 20–30 ppm. These results show that heteronuclear NMR spectroscopy may help to investigate silver pyrazolate/NHC complexes in solution and provides valuable structural information, although there is only a small number of reports on ¹J_{AgN} couplings²⁹ and ¹⁰⁹Ag chemical shifts^{5,27,30} so far.

Obviously, silver complexes of ligand precursors **1** show a well-balanced interplay of steric effects and bond strengths, and minor changes may have paramount effects on the resulting structures. Detailed knowledge of these effects is highly beneficial in the design of new ligands and complex molecular architectures.

Conclusion

A bulky tetradentate pyrazolate-bridged bis(NHC) ligand precursor **1b** was used to synthesize the structurally unprecedented octanuclear silver(I) complex **3**. Central and peripheral silver atoms are homoleptically coordinated to pyrazolate-N and NHC carbon atoms, respectively, thereby forming a “double-crown”-like structure. Stabilization of tetrameric pyrazolate coinage metal complexes by NHCs has not been reported before and may find an application in pyrazole chemistry. Furthermore, complexes **2–5** were investigated by NMR spectroscopy, which proved to be a powerful tool for characterization of these silver complexes. In order to get further insight in solution dynamics and the mechanism of conversion of **3** to **4** and **5**, investigations on related pyrazolate-bridged bis(NHC)-type ligands will be conducted in our laboratory.

Experimental Section

General Procedures. Melting points/decomposition temperatures were determined on an OptiMelt system (Stanford Research Systems, Inc.) using open capillaries; values are uncorrected. All NMR spectra were recorded on a Bruker Avance 500 MHz spectrometer in acetone-*d*₆ at -50 °C, unless indicated otherwise.

¹³C NMR resonances were obtained with proton broadband decoupling and referenced to the solvent septet of acetone-*d*₆ at 29.8 ppm (¹H 2.04 ppm). ¹⁵N and ¹⁰⁹Ag resonances were detected and assigned with HMQC-type schemes³¹ using transfer delays of 33 and 166 ms, respectively, and referenced to the unified Ξ scale³² using $\Xi(\text{Me}^{15}\text{NO}_2) = 10.136767$ and $\Xi(\text{sat. }^{109}\text{AgNO}_3) = 4.653533$. HMQC experiments with transfer delays of 33 ms were also used to assign the carbene and other quarternary carbon ¹³C resonances. Diffusion coefficients were measured at 25 °C with 2D DOSY experiments³³ using stimulated echo, bipolar sinusoidal 2.5 ms gradient pairs ramped in 128 steps from 1.1 to 50.4 G/cm and a diffusion delay (Δ) of 70 ms. Mass spectra were recorded using an Applied Biosystems API 2000 system. IR spectra from KBr pellets were recorded on a Digilab Excalibur Series FTS 3000 spectrometer. Elemental analyses were carried out by the analytical laboratory of the Institut für Anorganische Chemie der Universität Göttingen using an Elementar Vario EL III instrument.

Ligand precursors **1a,b** were prepared according to procedures recently developed;^{12,20} all other chemicals were purchased and used as supplied. All reactions were conducted under air.

General Procedure for the Preparation of Silver Complexes. Silver(I) oxide was added to a solution of the ligand precursor **1** in acetone, and the mixture was stirred at RT under exclusion of light. The reaction mixture was filtered over activated carbon and Celite 545, yielding a clear solution. Removal of the solvent under reduced pressure gave a crude product, and crystallization from acetone/diethyl ether yielded a first crop of colorless crystals of the silver complex. Further product can be obtained upon repeated crystallization.

Synthesis of 2. Starting materials: **1a** (1.08 g, 1.44 mmol), Ag₂O (0.73 g, 3.17 mmol), acetone (30 mL), reaction time 1 day. Crude product (light gray): 0.99 g. Crystallization using 126 mg of crude product in 10 mL of acetone gave a first crop of **2** (36.4 mg, 29%) as colorless crystals. Mp: 270 °C (dec). ¹H NMR (500 MHz, acetone-*d*₆, -50 °C): δ 1.80 (s, 6 H, *o*-CH₃), 1.97 (s, 6 H, *o*-CH₃), 2.27 (s, 6 H, *p*-CH₃), 5.21 (d, ²J_{HH} = 14.9 Hz, 2 H, CH₂), 5.63 (d, ²J_{HH} = 14.9 Hz, 2 H, CH₂), 6.62 (s, 1 H, CH^{Prz}), 7.00 (s, 2 H,

(31) Bax, A.; Griffey, R. H.; Hawkins, B. L. *J. Magn. Reson.* **1983**, *55*, 301–315.

(32) Harris, R. K.; Becker, E. D.; Cabral de Menezes, S. M.; Goodfellow, R.; Granger, P. *Pure Appl. Chem.* **2001**, *73*, 1795–1818.

(33) Morris, K. F.; Johnson, C. S. *J. Am. Chem. Soc.* **1992**, *114*, 3139–3141.

(29) Carmona, D.; Oro, L. A.; Lamata, M. P.; Jimeno, M. L.; Elguero, J.; Belguise, A.; Lux, P. *Inorg. Chem.* **1994**, *33*, 2196–2203.

(30) Bildstein, B.; Malaun, M.; Kopačka, H.; Wurst, K.; Mitterbock, M.; Ongania, K. H.; Opromolla, G.; Zanello, P. *Organometallics* **1999**, *18*, 4325–4336.

$CH^{ar-3,5}$, 7.04 (s, 2 H, $CH^{ar-3,5}$), 7.51 (s, 2 H, CH^{im}), 7.90 (s, 2 H, CH^{im}) ppm. ^{13}C NMR (125 MHz, acetone- d_6 , -50 °C): δ 17.7 (*o*- CH_3), 18.3 (*o*- CH_3), 20.8 (*p*- CH_3), 49.2 (CH_2), 104.1 (CH^{pz}), 122.9 (CH^{im}), 124.9 (CH^{im}), 129.7 ($CH^{ar-3,5}$), 129.8 ($CH^{ar-3,5}$), 135.1 ($CH^{ar-2,6}$), 135.2 ($CH^{ar-2,6}$), 136.9 (CH^{ar-1}), 139.8 (CH^{ar-4}), 152.3 ($C^{pz3,5}$), 177.6 (dd, $^1J_{^{13}C^{109}Ag} = 269.1$ Hz, $^1J_{^{13}C^{107}Ag} = 233.4$ Hz, Ag- C^{im}) ppm. ^{15}N NMR (51 MHz, acetone- d_6 , -50 °C): δ -182.2 (N^{im}), -181.3 (N^{im}), -109.4 (d, $^1J_{NAg} = 79$ Hz, N^{pz}) ppm. ^{109}Ag NMR (23 MHz, acetone- d_6 , -50 °C): δ 618.2 (N^{pz} -Ag- C^{im}) ppm. MS (ESI+): *m/z* (%) 678.8 (57, $[Ag_2L]^+$ and/or $[Ag_4L_2]^{2+}$), 572.8 (61, $[AgL]^+$ and/or $[Ag_2L_2]^{2+}$), 296.1 (51), 279.1 (55, $[C_{17}H_{19}N_4]^+$), 233.2 (100, $[H_2L]^{2+}$), 187.0 (46, $[C_{12}H_{15}N_2]^+$). MS (ESI-): *m/z* (%) 144.9 (100, $[PF_6]^-$). IR (KBr): 3433 (s, br), 3166 (w), 3138 (w), 2921 (m), 2853 (w), 1610 (m), 1489 (m), 1453 (m), 1410 (w), 1360 (w), 1280 (w), 1241 (w), 1195 (w), 1153 (w), 1113 (w), 1038 (m), 937 (w), 845 (vs), 766 (m), 747 (m), 682 (w), 557 (vs) cm^{-1} . Anal. Calcd for $C_{58}H_{62}Ag_4F_{12}N_{12}P_2$: C 42.26, H 3.79, N 10.20. Found: C 42.51, H 3.63, N 10.03.

Synthesis of 3. Starting materials: **1b** (1.50 g, 1.78 mmol), Ag_2O (1.03 g, 4.46 mmol), acetone (80 mL), reaction time 2 days. Crude product (brownish): 1.70 g. Crystallization using 150 mg of crude product in 5 mL of acetone gave a first crop of **3** (85.4 mg, 57%) as colorless crystals. Mp: 315 °C (dec). 1H NMR (500 MHz, acetone- d_6 , -50 °C): δ 0.17 (d, $^3J_{HH} = 6.8$ Hz, 3 H, CH_3), 0.38 (d, $^3J_{HH} = 6.8$ Hz, 3 H, CH_3), 0.86 (d, $^3J_{HH} = 6.8$ Hz, 3 H, CH_3), 0.92 (d, $^3J_{HH} = 6.8$ Hz, 3 H, CH_3), 1.06 (d, $^3J_{HH} = 6.8$ Hz, 3 H, CH_3), 1.08 (d, $^3J_{HH} = 6.8$ Hz, 3 H, CH_3), 1.13 (d, $^3J_{HH} = 6.8$ Hz, 3 H, CH_3), 1.16 (d, $^3J_{HH} = 6.8$ Hz, 3 H, CH_3), 1.74 (sept, $^3J_{HH} = 6.8$ Hz, 1 H, $CH(CH_3)_2$), 1.90 (sept, $^3J_{HH} = 6.8$ Hz, 1 H, $CH(CH_3)_2$), 2.20 (sept, $^3J_{HH} = 6.8$ Hz, 1 H, $CH(CH_3)_2$), 2.47 (sept, $^3J_{HH} = 6.8$ Hz, 1 H, $CH(CH_3)_2$), 5.49 (d, $^2J_{HH} = 14.2$ Hz, 1 H, CH_2), 5.84 (d, $^2J_{HH} = 14.2$ Hz, 1 H, CH_2), 6.07 (d, $^2J_{HH} = 14.2$ Hz, 1 H, CH_2), 6.13 (d, $^2J_{HH} = 14.2$ Hz, 1 H, CH_2), 6.58 (s, 1 H, CH^{pz}), 7.06 (d, $^3J_{HH} = 7.6$ Hz, 1 H, $CH^{ar-3,5}$), 7.09 (d, $^3J_{HH} = 7.6$ Hz, 1 H, $CH^{ar-3,5}$), 7.17 (d, $^3J_{HH} = 7.6$ Hz, 1 H, $CH^{ar-3,5}$), 7.30 (d, $^3J_{HH} = 7.6$ Hz, 1 H, $CH^{ar-3,5}$), 7.43 (t, $^3J_{HH} = 7.6$ Hz, 1 H, CH^{ar-4}), 7.46 (t, $^3J_{HH} = 7.6$ Hz, 1 H, CH^{ar-4}), 7.50 (m, 1 H, CH^{im}), 7.52 (m, 1 H, CH^{im}), 7.67 (m, 1 H, CH^{im}), 8.10 (m, 1 H, CH^{im}) ppm. ^{13}C NMR (125 MHz, acetone- d_6 , -50 °C): δ 23.2 (CH_3), 23.6 (CH_3), 23.7 (CH_3), 24.0 (CH_3), 24.6 (CH_3), 24.7 (CH_3), 25.2 (CH_3), 27.3 (CH_3), 28.3 ($CH(CH_3)_2$), 28.4 ($CH(CH_3)_2$), 28.6 ($CH(CH_3)_2$), 28.8 ($CH(CH_3)_2$), 49.4 (CH_2), 51.5 (CH_2), 104.2 (CH^{pz}), 121.5 (CH^{im}), 124.0 (CH^{im}), 124.4 ($CH^{ar-3,5}$), 124.4 ($CH^{ar-3,5}$), 124.4 ($CH^{ar-3,5}$), 124.6 ($CH^{ar-3,5}$), 124.7 (CH^{im}), 125.9 (CH^{im}), 130.9 (CH^{ar-4}), 131.0 (CH^{ar-4}), 134.9 (CH^{ar-1}), 135.3 (CH^{ar-1}), 144.9 ($CH^{ar-2,6}$), 144.9 ($CH^{ar-2,6}$), 146.1 ($CH^{ar-2,6}$), 146.4 ($CH^{ar-2,6}$), 149.2 ($C^{pz3,5}$), 153.7 ($C^{pz3,5}$), 180.0 (dd, $^1J_{^{13}C^{109}Ag} = 209.5$ Hz, $^1J_{^{13}C^{107}Ag} = 180.8$ Hz, Ag- C^{im}), 183.4 (dd, $^1J_{^{13}C^{109}Ag} = 211.1$ Hz, $^1J_{^{13}C^{107}Ag} = 183.3$ Hz, Ag- C^{im}) ppm. ^{15}N NMR (51 MHz, acetone- d_6 , -50 °C): δ -187.0

(N^{im}), -183.2 (N^{im}), -183.1 (N^{im}), -180.2 (N^{im}), -117.6 (d, $^1J_{NAg} = 97$ Hz, N^{pz}), -116.4 (d, $^1J_{NAg} = 97$ Hz, N^{pz}) ppm. ^{31}P NMR (202 MHz, acetone- d_6 , -50 °C): δ -144.3 (sept, $^1J_{^{19}F^{31}P} = 709$ Hz, PF_6) ppm. ^{109}Ag NMR (23 MHz, acetone- d_6 , -50 °C): δ 469.7 (N^{pz} -Ag- N^{pz}), 636.5 (C^{im} -Ag- C^{im}) ppm. MS (ESI+): *m/z* (%) 1671.3 (5, $[Ag_4L_2PF_6]^+$ and/or $[Ag_8L_4(PF_6)_2]^{2+}$), 1561.3 (3), 1419.5 (4, $[Ag_3L_2]^+$ and/or $[Ag_6L_4]^{2+}$), 762.7 (100, $[Ag_2L]^+$ and/or $[Ag_4L_2]^{2+}$ and/or $[Ag_8L_4]^{4+}$), 655.2 (23, $[AgL]^+$), 107.0 (19, $[Ag]^+$). MS (ESI-): *m/z* (%) 145 (100, $[PF_6]^-$). IR (KBr): 3437 (m, br), 3171 (m), 3142 (m), 3073 (w), 2965 (s), 2934 (s), 2871 (s), 1713 (m), 1679 (m), 1623 (m), 1594 (m), 1561 (m), 1521 (w), 1471 (s), 1461 (s), 1414 (s), 1386 (w), 1365 (s), 1333 (w), 1308 (m), 1272 (w), 1248 (m), 1223 (s), 1182 (m), 1150 (w), 1121 (m), 1108 (m), 1059 (m), 1041 (w), 960 (m), 937 (m), 843 (vs), 808 (s), 762 (s), 740 (s), 689 (m), 636 (w), 617 (w), 558 (vs), 469 (w) cm^{-1} . Anal. Calcd for $C_{140}H_{172}Ag_8F_{24}N_{24}P_4 \cdot 2C_3H_6O$: C 46.76, H 4.95, N 8.96. Found: C 46.66, H 4.97, N 8.64.

X-ray Crystallography. Crystal data and details of the data collections for **2** and **3** are given in Table 2. X-ray data were collected on a STOE IPDS II diffractometer (graphite-monochromated Mo K α radiation, $\lambda = 0.71073$ Å) by use of ω scans at -140 °C. The structures were solved by direct methods and refined on F^2 using all reflections with SHELX-97.³⁴ Most non-hydrogen atoms were refined anisotropically. Hydrogen atoms were placed in calculated positions and assigned to an isotropic displacement parameter of 0.08 Å². Two PF_6^- anions in **3** were found to be disordered and were refined using SADI restraints (d_{p-F} and $d_{F...F}$) and EADP constraints. The unit cell of **3** contains disordered diethyl ether and acetone solvent molecules that occupy an area of 2077.2 Å³ (22.2%). No satisfactory model for the disorder could be found, and for further refinement the contribution of the missing solvent molecule (total electron count 518) was subtracted from the reflection data by the SQUEEZE³⁵ routine of the PLATON³⁶ program. A face-indexed absorption correction for **2** was performed numerically with the program X-RED.³⁷

Acknowledgment. Financial support by the Fonds der Chemischen Industrie is gratefully acknowledged.

Supporting Information Available: Crystal data (CIF file) and ORTEP plots for **2** and **3**. NMR data of **3**, **4**, and **5** at RT. Variable-temperature 1H NMR spectra. This material is available free of charge via the Internet at <http://pubs.acs.org>.

OM800487E

(34) Sheldrick, G. M. *Acta Crystallogr.* **2008**, *A64*, 112–122.

(35) van der Sluis, P.; Spek, A. L. *Acta Crystallogr.* **1990**, *A46*, 194–201.

(36) Spek, A. L. *Acta Crystallogr.* **1990**, *A46*, C34.

(37) GmbH, S. C. *X-RED*; STOE & CIE GmbH: Darmstadt, 2002.